

Article

Proton Generation Using Chitin–Chitinase and Collagen–Collagenase Composites

Hitoki Semizo *, Ryusei Yabu and Yasumitsu Matsuo *

Faculty of Science & Engineering, Setsunan University, Ikeda-Nakamachi, Neyagawa 572-8508, Japan;
22m912yr@edu.setsunan.ac.jp

* Correspondence: 20d904sh@edu.setsunan.ac.jp (H.S.); ymatsuo@lif.setsunan.ac.jp (Y.M.)

Abstract: Hydrogen energy is focused on as next-generation energy without environmental load. Therefore, hydrogen production without using fossil fuels is a key factor in the progress of hydrogen energy. In the present work, it was found that chitin–chitinase and collagen–collagenase composites can generate protons by the hydrolysis of the enzyme. The concentration of the generated proton in the chitin–chitinase and collagen–collagenase composites are $1.68 \times 10^{17} \text{ cm}^{-3}$ and $1.02 \times 10^{17} \text{ cm}^{-3}$, respectively. Accompanying these results, proton diffusion constants in the chitin and collagen membranes are also estimated to be $8.59 \times 10^{-8} \text{ cm}^2/\text{s}$ and $8.69 \times 10^{-8} \text{ cm}^2/\text{s}$, respectively. Furthermore, we have fabricated the bio-fuel cell using these composites as hydrogen fuel and demonstrated that these composites become a fuel of the fuel cell.

Keywords: biomaterials; enzyme; proton conductivity; amperometry



Citation: Semizo, H.; Yabu, R.; Matsuo, Y. Proton Generation Using Chitin–Chitinase and Collagen–Collagenase Composites. *J. Compos. Sci.* **2022**, *6*, 166. <https://doi.org/10.3390/jcs6060166>

Academic Editor: Francesco Tornabene

Received: 21 April 2022

Accepted: 6 June 2022

Published: 7 June 2022

Publisher's Note: MDPI stays neutral with regard to jurisdictional claims in published maps and institutional affiliations.



Copyright: © 2022 by the authors. Licensee MDPI, Basel, Switzerland. This article is an open access article distributed under the terms and conditions of the Creative Commons Attribution (CC BY) license (<https://creativecommons.org/licenses/by/4.0/>).

1. Introduction

Hydrogen energy is important as next-generation energy with no environmental load. Therefore, hydrogen production is important, and much research has been done. For example, Dicks et al. reported how to use natural gas to produce hydrogen [1]. Möller et al. suggested the possibility of converting natural gas to hydrogen using solar steam reforming [2]. Lefebvre et al. also reported that AlO–ZrO-supported nickel-alumina spinel could be used as a catalyst for steam reforming to generate hydrogen [3]. However, currently, most hydrogen production depends on fossil fuels. Since fossil fuels have problems of depletion and carbon dioxide emissions, it is necessary to present hydrogen production without using fossil fuels. Biomaterials are also suitable in terms of carbon neutrality. For example, Takahashi et al. suggested that hydrogen is produced from the photosystem II (PSII) of plants [4]. Hosseini et al. also attempted to generate hydrogens from supercritical water gasification (SCWG) of biomass [5]. In this way, the biomaterial is an attractive material for hydrogen production without environmental load. It is also known that the solution to the environmental pollution by the discarded plastics called the “microplastic problem” is desired. Andrady, A, L described the “microplastic problem” where microplastics cause marine pollution [6]. Cauwenberghe et al. also reported the effects of microplastics on the human body [7]. Bilo et al. suggested that bioplastics are produced from rice straw [8]. Maheswari et al. also indicated the use of *Spirulina platensis* to introduce new bioplastics [9]. In addition, Moorthy et al. suggested the possibility of a film blended with polyvinyl alcohol and spirulina algae with higher biodegradability [10]. In this way, the biosystem is an environmentally friendly one and is a useful system if it can be used for hydrogen generation.

From the viewpoint of the hydrogen ion (proton) transport, Dellago et al. described the diffusion of protons through water-filled carbon nanotubes [11]. Proton transport capacity is important when materials are used as electronic devices. Recently, some research on proton transport of biomaterials has been conducted. Chitin is a biomaterial with the chemical formula of $(\text{C}_8\text{H}_{13}\text{O}_5\text{N})_n$ and consists of long chains of N-acetylglucosamine.

Shibata et al. reported on an epoxy/chitin nanofiber composite with hardened chitin [12]. Kawabata et al. have shown that chitin has a proton transport capacity and can be applied to fuel cell electrolytes [13]. As described above, chitin has been put into practical use in many fields such as biotechnology, pharmacy, agriculture, food engineering, environmental technology, textile, and paper manufacturing industries. Collagen is a biological substance consisting of amino acids such as glycine and proline and is also known as the main component of fish scales. Matsui et al. suggest that the biomaterial “collagen” becomes a proton conductor by hydration [14]. Furthermore, Matsuo et al. clarified that collagen could be applied as a fuel cell electrolyte [15]. In addition, Matsuo et al. have created a DNA thin film and are trying to apply it to a fuel cell electrolyte [16]. Furuseki et al. described squid axonal electrolytes and their proton conductivity [17]. Thus, biomaterials become excellent proton transporters.

In recent years, research has also been conducted on applying biological substances to devices. Zhong et al. were trying to create a bio-device using polysaccharides [18]. In addition, Park et al. reported on bio-FETs using DNA [19]. However, since rare metals are used for hydrogen production, there are problems of cost and resource depletion. Therefore, biomaterials that realize both proton conduction and proton generation contribute to cheaper and better applications to devices. The enzyme, which is one of the biomaterials, is known as an excellent catalyst. Kirk reported on the industrial use of enzymes in various fields [20]. In addition, Galan et al. reported on application examples of enzymes in the energy field [21]. Among them, various applications of hydrolases have been reported. Sathya et al. reported on the diversity of meta-genomic-derived glycosyl hydrolases and their application to the food industry [22]. Imig et al. described the application of soluble epoxide hydrolases to the medical field [23]. Liu et al. have attempted to characterize the structural and functional properties of polyethylene terephthalate hydrolases [24]. Hydrolases can be genetically modified to improve their activity. Chitinase and collagenase are known as hydrolases that hydrolyze biomaterials. Arakane et al. reported that insect chitinase is an endotype hydrolase [25]. In addition, Perrakis et al. clarified the crystal structure of bacterial chitinase [26]. Furthermore, Fukamizo reported the catalytic action of Chitinolytic enzymes [27]. In addition, Welgus et al. showed the collagen substrate specificity of human skin fibroblast collagenase [28]. Daboor et al. extracted and purified collagenase enzymes for industrial use [29]. In addition, Souza et al. reported the catalytic mechanism of collagenase [30]. Thus, chitinase and collagenase are the enzymes of interest and are known as excellent catalysts.

Recently, we have found that chitin–chitinase and collagen–collagenase composites can generate protons. Enzyme-based proton production does not need to be fixed in terms of proton conductivity, and since both are biomaterials, good consistency is also an advantage. Karthikeyan et al. reported the influence of chitosan substrate and its nanometric form on the green power generation in sediment microbial fuel cells [31]. This paper reports on these results. In addition, we have determined the values of the diffusion constants of protons in collagen and chitin. This result will help lead to the next generation of new proton production methods.

2. Materials and Methods

2.1. Preparation of Chitin–Chitinase Composite

Chitin membranes were prepared by aspiration filtration at room temperature using purified chitin slurry (Sugino Machine Limited, Uozu, Japan) dispersed in distilled water. For suction filtration, a PTFE hydrophilic filter with 0.2 μm diameter holes was used. Figure 1 shows a photograph of the prepared chitin membrane, which is a cloudy and mechanically stable film. The dimensions of the chitin membrane used in this study are ϕ 4.5 \times 0.07 mm, as shown in Figure 1. Under humidified conditions, chitin also shows proton conductivity. The value of proton conductivity increases with increasing humidity and becomes $\sim 1 \times 10^{-2}$ S/m under 100% humidified conditions [13]. The chitin membrane is stable up to 200 °C. The chitinase used in this study is of activity of 110 units/mL (FUJIFILM

Wako Pure Chemical Corporation, Osaka, Japan). Proton production was carried out by coating the chitin membrane with the chitinase. The proton concentrations predicted from the mechanism are 2.36×10^{21} .



Figure 1. Chitin membrane.

2.2. Preparation of Collagen–Collagenase Composite

Figure 2 shows a collagen membrane grown from the purified collagen peptide (UNIQS Co. Ltd., Yokohama, Japan). The dimensions of the collagen membrane used in this study are $\phi 4.5 \times 0.05$ mm. As shown in Figure 2, the collagen film is transparent. Under the humidified condition, the collagen exhibits proton conductivity by the transfer of protons (or H_3O^+) through the water bridges formed between the OH, CO, and NH groups of the side chains of the collagen peptide. The value of proton conductivity of the collagen is $\sim 1 \times 10^{-3}$ S/m under 100% [14]. The collagen membrane is stable up to 160 °C. The collagenase used in this study is of activity of 290 units/mg (FUJIFILM Wako Pure Chemical Corporation). Protons were generated by coating the collagen membrane with the collagenase. The proton concentrations predicted from the mechanism are 2.21×10^{24} .

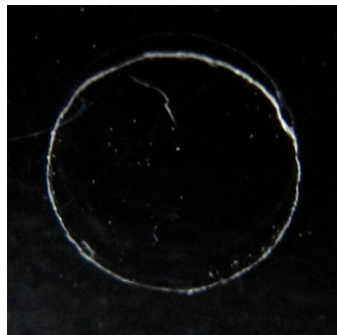


Figure 2. Collagen membrane.

2.3. Amperometric Measurements

The purpose of this study is to investigate the carrier generation when the enzyme chitinase is applied to the chitin membrane. The generation and diffusion of carriers can be studied by various methods, but in this study, we will use amperometry, which is simple and quick to measure [32–35]. In this study, we use amperometry, which is a simple and quick method. Amperometry is a method to investigate the carrier transport that occurs when a step voltage is applied to a sample from the transient current [36–39]. The application of a step voltage to the sample polarizes the internal charge and transports the charge, which is the conduction carrier, to a stable position (near the electrode). As a result, we can obtain information about the carrier from the transient current. The measurement system is very simple (Figure 3), requiring only a DC power supply to apply the step voltage, an ammeter to measure the current, and a computer to control them. In this study, a DC stabilized power supply (keithley2400) was used as a DC power supply to apply a step voltage, and the current was measured by a high precision digital multimeter (keithley2100)

at room temperature. The chitin and collagen membranes with the dimensions shown in the previous section were used for the measurements, and silver electrodes were applied to those for the measurements. The complex was obtained by placing the membrane in enzyme vapor and injecting it into chitin (collagen).

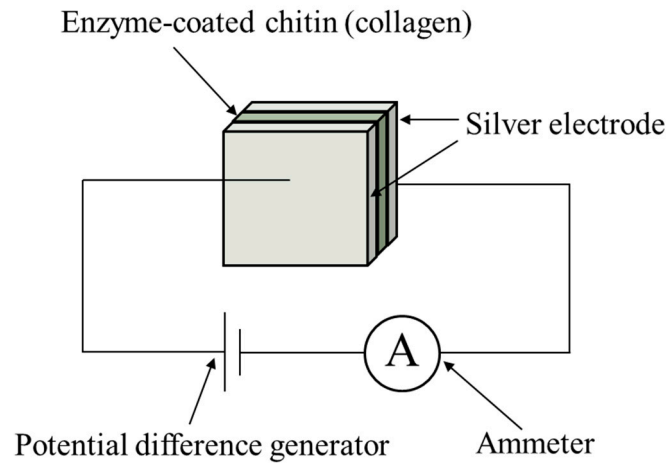


Figure 3. Amperometry measurement system.

2.4. Bio-Fuel Cells Using the Chitin–Chitinase and Collagen–Collagenase Composites as Fuel

In this section, we have fabricated the bio-fuel cell using the chitin–chitinase and collage–collagenase composite as fuel and displayed that the chitin–chitinase and collagen–collagenase composites become hydrogen fuels. We first explain the structure of the bio-fuel cells. Figure 4 shows the schematic figure of the structure of the bio-fuel cell. As shown in Figure 4, the chitin membrane was used as the fuel–cell electrolyte. The Pt–C electrodes sandwiched the electrolyte, and chitin–chitinase (or collagen–collagenase) composite as anode fuel was used. The oxygen in the air was introduced to the cathode as a fuel. The stainless mesh was used as the current collector, and the generated current was measured between the stainless-mesh current collectors of anode and cathode in the bio-fuel cell. The electrode area was $1.59 \times 10^{-5} \text{ m}^2$, and the measurement was carried out under humidified conditions.

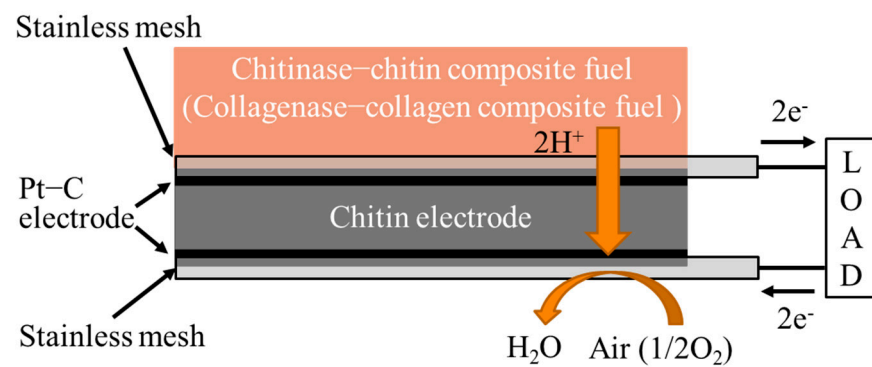


Figure 4. Structure of bio-fuel cell.

In the fuel cell characteristic measurement, the conditions of temperature, enzyme activity, and film thickness are the same as the conditions of amperometric measurements, and it is a highly biocompatible device. In this study, the current–voltage characteristics were measured by a precision digital multimeter (keithley2100).

3. Results and Discussion

3.1. Carrier Production in Chitin–Chitinase Composites

The simplest way to obtain information about the carriers produced by the enzyme is to measure the change in the current flowing through the sample. As is well known, transient changes in current can be known by amperometry. Therefore, we first investigated the transient current changes of a well-known polysaccharide and its enzyme, chitin–chitinase composite. Figure 5 shows the current value at each applied voltage. From Figure 5, the maximum voltage in the range not affected by water splitting is 0.8V, and this time, the transient current was measured when 0.8V was applied.

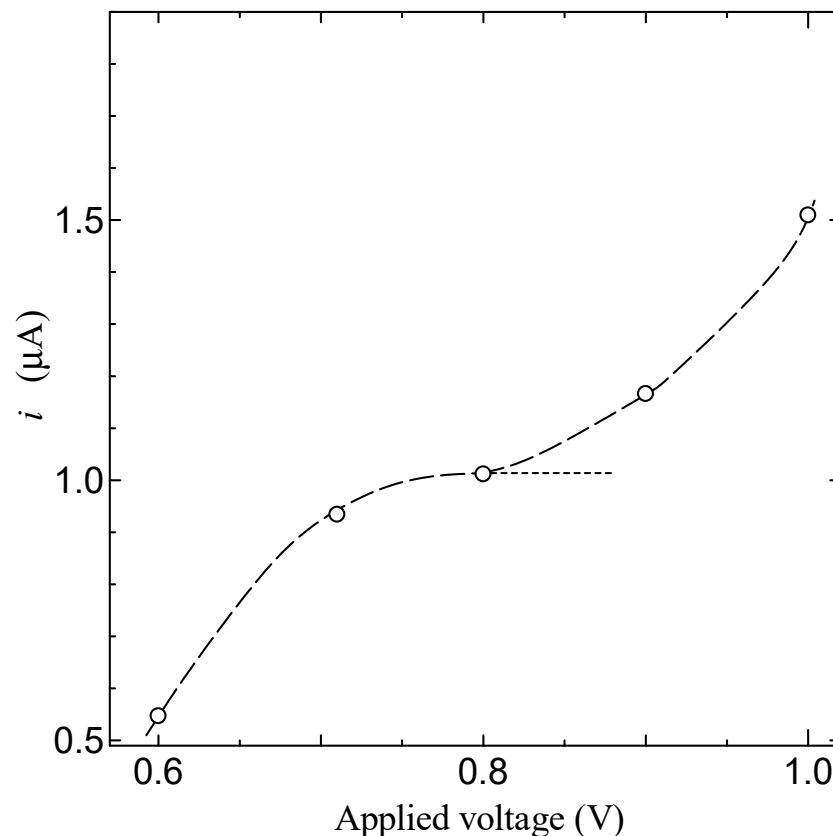


Figure 5. Current value at each applied voltage.

Figure 6 shows the results of the measurements. In this measurement, the step voltage of 0.8 V was applied as the value at which the transient currents of chitin and chitin–chitinase composite coincide at $t \rightarrow \infty$. As shown in Figure 6, both the collagen and chitin–chitinase composite exhibit so-called “transient currents” in which the current value increases once and then slowly decays after the step voltage is applied.

The behaviors of these transient currents are very similar, suggesting that the transient currents in the chitin and chitin–chitinase composite decay by the same mechanism. These results suggest that there is a current generated by the carriers produced in the chitin–chitinase composite. Considering that the chitin membrane is a proton conductor upon hydration, as shown in Figure 6, it is suggested that the transient currents are caused by the diffusion of protons in the chitin and chitin–chitinase membrane.

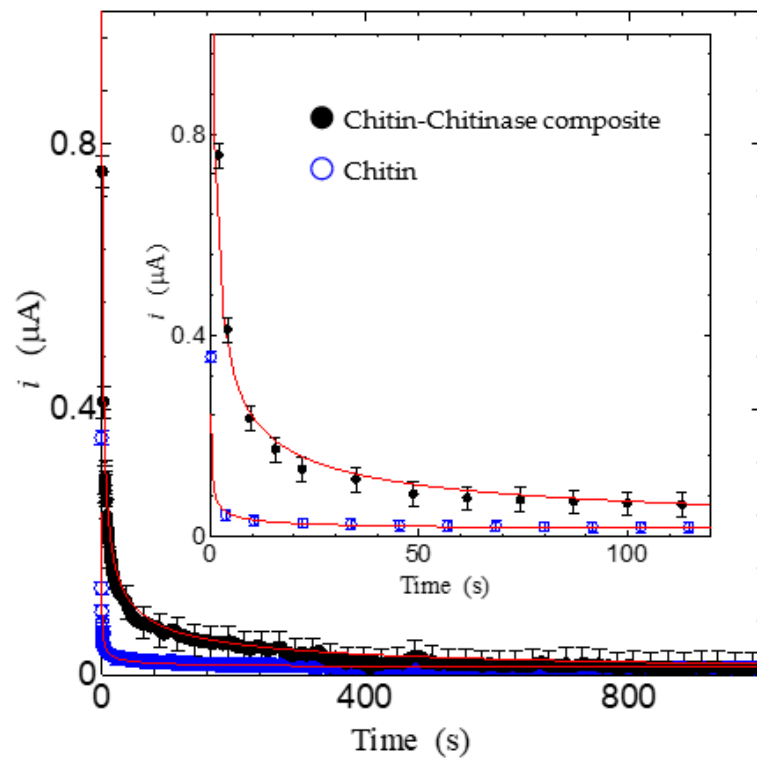


Figure 6. Time dependence of transient current after applying step voltage of 0.8 V. The inset shows the enlarged data.

The transient current due to carrier diffusion has already been analyzed in various methods and can be understood by solving the diffusion equation. The diffusion of ions due to transient currents is described by Fick’s first law as follows:

$$i = nFAD_o \left(\frac{\partial C_o}{\partial x} \right)_{x=0} \tag{1}$$

Here, n is the charge number, F is a Faraday constant that represents the charge per amount of substance of an electron ($9.6485 \times 10^4 \text{ C/mol}$), A is the electrode area, and D_o and C_o are the diffusion constant and carrier concentration, respectively. The symbol x is the distance measured from the electrode interface to the bulk of the sample. The carrier concentration gradient part of this equation can be solved by setting the diffusion equation as $C = C_o$ for initial conditions $t = 0$ and $x \geq 0$, $C = 0$ for boundary conditions $x = 0$, and $C \rightarrow C_o$ for $x \rightarrow \infty$, using the error function erf, can be obtained as the following equation,

$$c(t, x) = C_o \text{erf} \left(\frac{x}{2(D_o t)^{1/2}} \right) \tag{2}$$

Differentiating this and substituting it into Equation (1), we obtain the following equation,

$$i = \frac{nFAD_o C_o}{(\pi D_o t)^{1/2}} \tag{3}$$

This equation is known as Cottrell’s equation, and it shows that the diffusion current (transient current) at a flat electrode is inversely proportional to the square root of time. The solid line in Figure 6 shows the result calculated by the Cottrell equation in Equation (3). As shown in the solid line in Figure 6, the transient currents of both chitin membrane and chitin–chitinase composite decrease at $t^{-1/2}$ according to Cottrell’s equation. These results suggest that carrier diffusion is the cause of these transient currents in Figure 6.

Although the carrier concentration C_o and the diffusion constant D_o cannot be obtained separately, the product of these two, $C_o D_o^{1/2}$, can be obtained directly from the experimental result. The $C_o D_o^{1/2}$ of chitin membrane and chitin–chitinase composite were found to be 1.60×10^{-11} and 8.70×10^{-11} mol/cm²·s^{-1/2}, respectively. This is an important value for determining proton transport, and we can uniquely determine the diffusion constant and carrier concentration in the system if the value of C_o or D_o is obtained. As is well known, enzymes are catalysts, and the enzyme itself does not change between the starting and ending states of the reaction but plays a role in promoting the reaction. The chitinase used in this study plays a role in breaking the glycosidic bonds between chitin molecules by hydrolysis. Figure 7 shows the schematic diagram. As shown in Figure 7, when the enzyme chitinase encounters chitin, the glycosidic bond between the chitin molecules is broken, and with the intervention of water, an OH group is attached to the C that formed the glycosidic bond. Thus, the enzymatic breaking of the glycosidic bond gives rise to a new OH group. Furthermore, as is well known, the protons of the OH groups of the side chains are detached from the OH groups. This result suggests that chitinase, known as a hydrolytic enzyme, plays a role in increasing the number of protons by generating new protons which are carriers in chitin. In other words, considering that the main effect of chitinase on proton transport is to increase the number of protons, we can assume that the main contribution to the increase of transient current in chitin–chitinase composite is not the change of the diffusion constant but the change of carrier concentration.

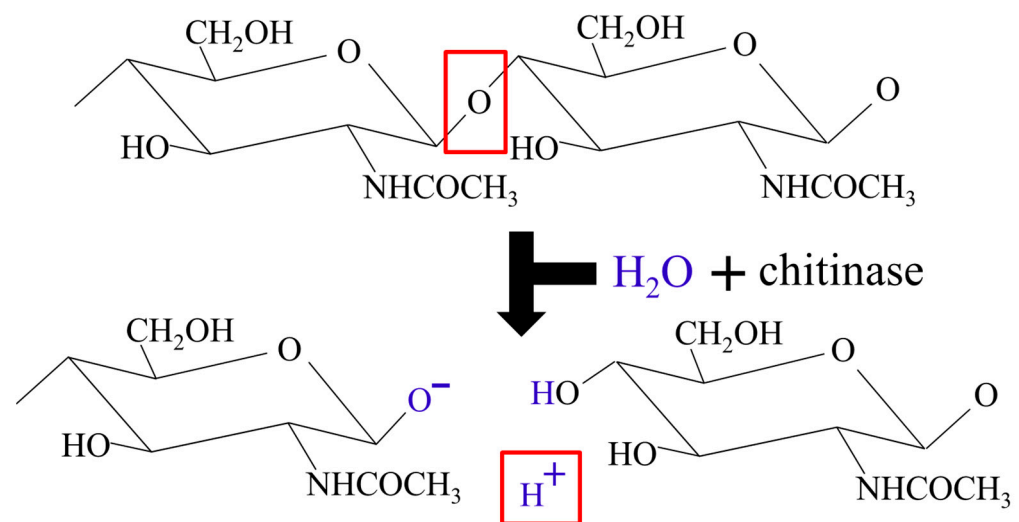


Figure 7. Cleavage of chitin glycosidic bonds by chitinase.

Therefore, assuming that the change in diffusion constant due to chitinase is negligible, the concentration of carriers generated in chitin by chitinase can be roughly estimated from the measurement results shown in Figure 6. The product of the carrier concentration and the diffusion constant of the chitin and the chitin–chitinase composite is $C_{oc} D_{oc}^{1/2}$ and $C_{oe} D_{oe}^{1/2}$, respectively. Using the condition $D_{oc} = D_{oe} (=D_o)$ for the diffusion constant, the carrier concentration C_{oe} produced in the chitin–chitinase composite is 5.4 times higher than the carrier concentration C_{oc} in the chitin membrane. This result also suggests that C_{oc} , C_{oe} , and D_o can be uniquely determined if another relation for C_{oc} and C_{oe} can be obtained. Therefore, we further analyzed the difference in transient currents between the chitin membrane and the chitin–chitinase composite. The results are shown in Figure 8.

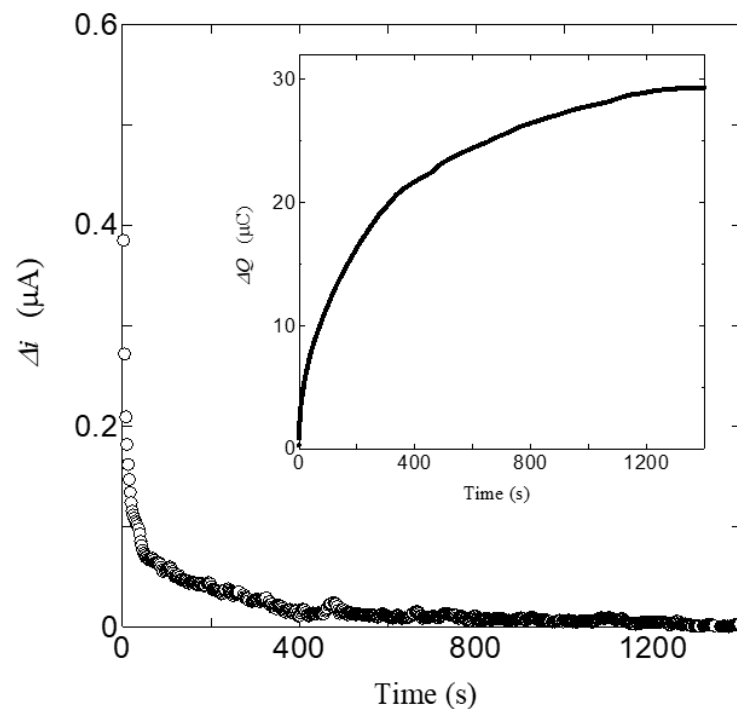


Figure 8. Time dependence of Δi . Inset is Time dependence of ΔQ .

As shown in Figure 8, the difference in transient currents between the chitin membrane and the chitin–chitinase composite, Δi , decreases rapidly with time. The time variation of the charge generated by the chitin–chitinase composite can be obtained by integrating the results of Figure 8. The time dependence is shown in the inset of Figure 8. As shown in this figure, the current-generating almost saturates around 400 s. It is suggested that this result is caused by the transport of protons generated by chitinase. Therefore, the number of carriers generated in the chitin–chitinase composite can be obtained by dividing the saturation charge by the charge element. The difference in carrier concentration between the chitin membrane and the chitin–chitinase composite is $1.68 \times 10^{17} \text{ cm}^{-3}$, taking into account the volume of the chitin membrane. Using these values, C_{oc} , C_{oe} , and D_o are estimated to be $(1.84 \pm 0.0155) \times 10^{16} \text{ cm}^{-3}$, $(1.86 \pm 0.0172) \times 10^{17} \text{ cm}^{-3}$, and $(8.59 \pm 0.0159) \times 10^{-8} \text{ cm}^2/\text{s}$, respectively. The maximum carrier concentration due to the enzymatic reaction in the chitin–chitinase complex is estimated. The estimated concentration is $2.17 \times 10^{21} \text{ cm}^{-3}$. This result indicates that a part of protons in the chitin–chitinase composite contributes to proton conduction. In addition, Hirota et al. show that the diffusion constant in chitin is $\sim 3 \times 10^{-7} \text{ cm}^2/\text{s}$ at 268 K by the neutron quasi-elastic scattering (QENS) measurement [40]. The diffusion constant in this work is close to the diffusion constant obtained by the QENS measurement. The diffusion constant estimated from the QENS measurement is a microscopic diffusion constant, which includes the diffusion at a distance of several micrometers or less. On the other hand, the diffusion constant in this study is a macroscopic diffusion constant, which is determined by the total amount of carrier migration. It is generally suggested that the diffusion constant, including the microscopic diffusion, could be larger than the macroscopic diffusion constant [41]. Considering these, the diffusion constant obtained in this work is reasonable.

3.2. Carrier Production in Collagen–Collagenase Composites

Collagen and collagenase are also a well-known protein and enzyme. In this section, we show the investigation of the carrier concentration and diffusion constant in the collagen membrane and collagen–collagenase composite using the protein and its enzyme. Figure 9 shows the time dependence of transient currents in the collagen membrane and collagen–collagenase composite.

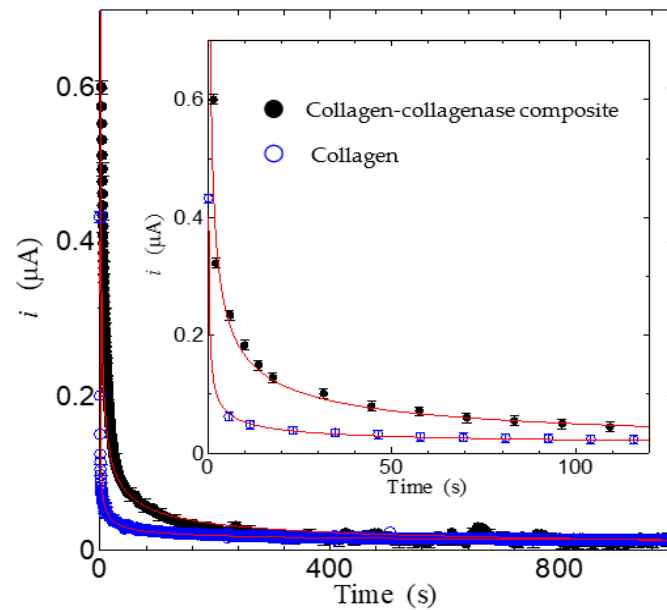


Figure 9. Time dependence of transient current after applying step voltage of 0.8 V. The inset shows the enlarged data.

In this measurement, the applied voltage 0.8 V was determined as the value at which the transient currents of collagen and collagen–collagenase composite coincide at $t \rightarrow \infty$. As shown in Figure 9, the behaviors of these transient currents are similar to transient currents in the chitin membrane and chitin–chitinase composite. These results indicate that the transient currents in the collagen membrane and collagen–collagenase composite are not caused by the discharging of the electric double layer but by the proton diffusion, as seen in the chitin membrane and chitin–chitinase composite. The solid line in Figure 9 shows the result of checking whether the measurement results in Figure 9 can be described by the Cottrell equation in Equation (3). As shown in the solid line in Figure 9, the transient currents of both collagen and collagenase–collagen membranes decrease at $t^{-1/2}$ according to Cottrell’s equation. These results suggest that transient current in the collagen membrane and collagen–collagenase is also caused by the carrier diffusion. From these results, the $C_0 D_0^{1/2}$ of collagen and collagenase–collagen membranes were found to be 1.60×10^{-11} and $6.60 \times 10^{-11} \text{ mol/cm}^2 \cdot \text{s}^{-1/2}$, respectively.

Collagenase used in this study plays a role in breaking the amide bonds between collagen molecules by hydrolysis. Figure 10 shows the schematic figure of the reaction by collagenase. As shown in Figure 10, when the enzyme collagenase encounters collagen, the amide bond between the collagen molecules is broken, and with the intervention of water, an OH group is attached to the Carbon that forms the amide bond. Thus, the enzymatic breaking of the amide bond gives rise to a new OH group. As is well known, the protons of the OH groups of the side chains are detached from the OH groups when under humidified conditions. This result suggests that collagenase, a hydrolytic enzyme, plays a role in increasing the number of protons by generating new protons, which are carriers of collagen. Assuming that the change in diffusion constant due to collagenase is negligible, same as the case of chitinase, the concentration of carriers generated in collagen by collagenase can be roughly estimated from the measurement results shown in Figure 9. Figure 11 shows the difference in transient currents between the collagen membrane and the collagen–collagenase composite. As shown in Figure 11, the difference in transient currents between the collagen membrane and the collagen–collagenase membrane, Δi , decreases rapidly with time. The time dependence of the charge generated by the collagen–collagenase is shown in the inset of Figure 11. As shown in the inset of Figure 11, the total generated carrier charge obtains from the saturation value of around 400 s. From these results, the difference in carrier concentration between the collagen membrane and the collagenase–collagen

membrane is $1.02 \times 10^{17} \text{ cm}^{-3}$, taking into account the volume of the collagen membrane. Using these values, C_{oc} , C_{oe} , and D_0 are estimated to be $(3.27 \pm 0.0481) \times 10^{16} \text{ cm}^{-3}$, $(1.35 \pm 0.0209) \times 10^{17} \text{ cm}^{-3}$, and $(8.69 \pm 0.0269) \times 10^{-8} \text{ cm}^2/\text{s}$, respectively. The maximum carrier concentration of the collagen–collagenase complex due to the enzymatic reaction is estimated to be $1.33 \times 10^{21} \text{ cm}^{-3}$. These results also indicate that a part of protons in the collagen–collagenase composite yields proton conduction.

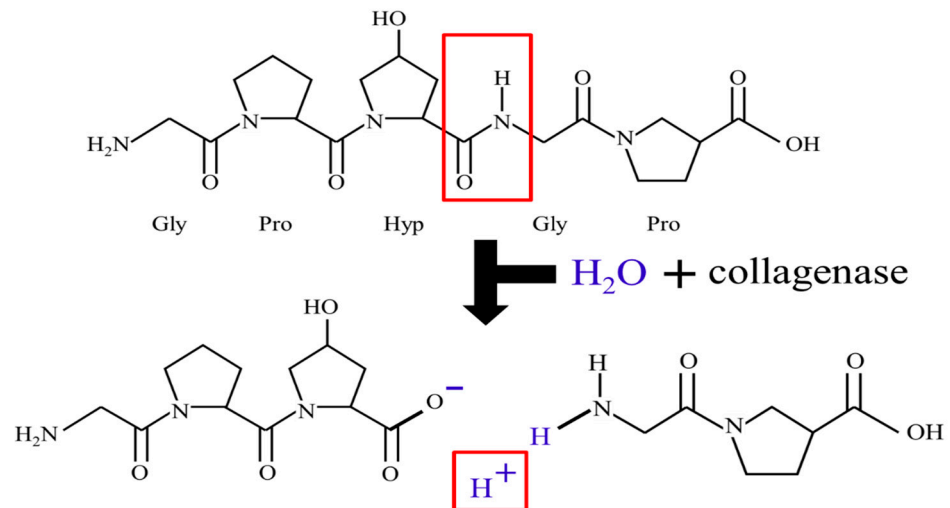


Figure 10. Cleavage of collagen amide bonds by collagenase.

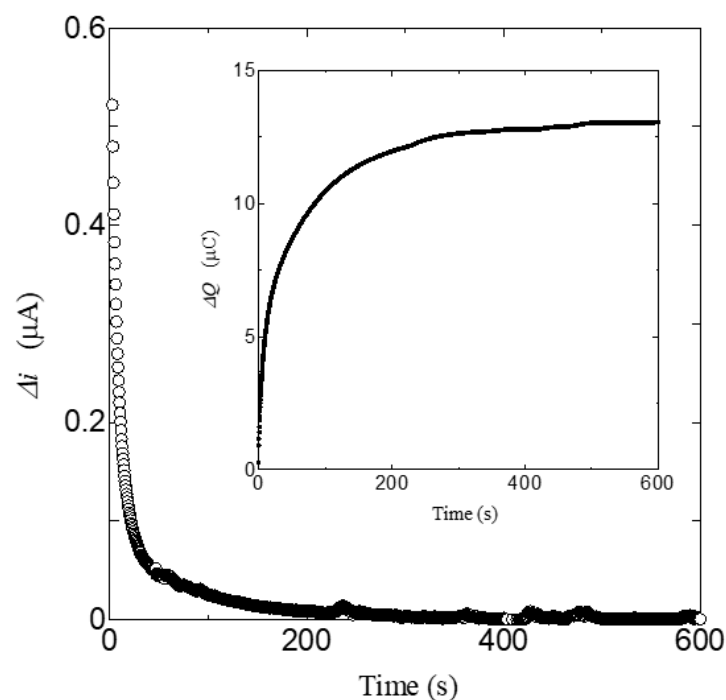


Figure 11. Time dependence of Δi . Inset is time dependence of ΔQ .

3.3. Bio-Fuel Cells Using the Chitin–Chitinase and Collagen–Collagenase Composites as Fuel

Figure 12 shows the relationship between the current density and cell voltage of the bio-fuel cell using chitin–chitinase fuel and collagen–collagenase fuel, respectively. As shown in Figure 12, both the current–cell voltage curves using the chitin–chitinase fuel and the collagen–collagenase fuel exhibit the typical current–cell voltage characteristic feature in which the current density decreases with increasing the cell voltage. These results indicate that chitin–chitinase composite and collagen–collagenase composite become the

fuel of the fuel cell. That is, chitin–chitinase and collagen–collagenase composites generate protons and become the fuel of the fuel cell.

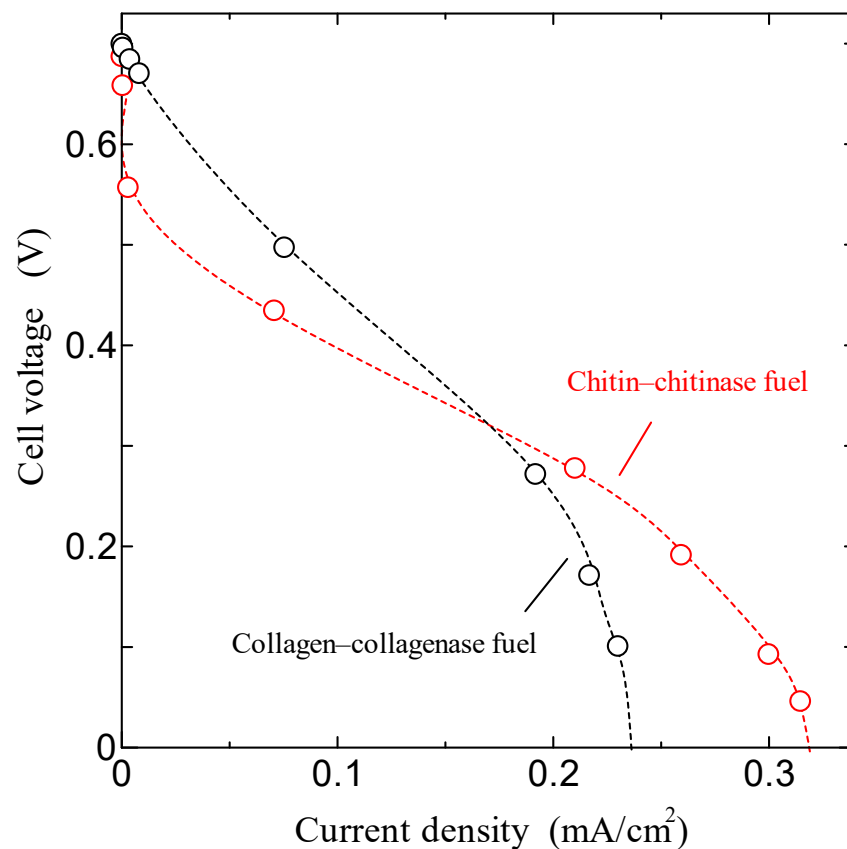


Figure 12. Current–cell voltage relation in the bio-fuel cell using the chitin–chitinase fuel and the collagen–collagenase fuel.

In order to estimate the amount of the generated hydrogen roughly, we calculate the proton concentration from Figure 12. The proton concentration can be calculated by extrapolating the current–cell voltage curve to the current density axis using Faraday’s second law roughly. The current i_0 obtained from the extrapolated current–cell voltage curve is expressed with the following equation, $i_0 = zmF$. Here, F is the Faraday constant, and m and z are the proton concentration per unit time and the charge number of a proton, respectively. Using this equation and the dimensions of the chitin–chitinase and collagen–collagenase composites, we can calculate the proton concentration m to be $2.77 \times 10^{17} \text{ cm}^{-3}$ for the chitin–chitinase composite and $2.73 \times 10^{17} \text{ cm}^{-3}$ for the collagen–collagenase composite. These proton concentrations are in good agreement with $1.86 \times 10^{17} \text{ cm}^{-3}$, and $1.35 \times 10^{17} \text{ cm}^{-3}$ obtained from the transient currents in Sections 3.1 and 3.2. These results indicate that the concentration and diffusion constants obtained in Sections 3.1 and 3.2 are reasonable. In the present work, we can introduce that the substrate–enzyme composite becomes a proton source and can be used as the fuel of fuel cells. In addition, by using enzymatic carrier generation, the carrier concentration and diffusion constant can be estimated by measuring the difference in transient currents. It is well-known that there are a lot of enzymes. We plan to research the combination between substrate and enzyme with a lot of hydrogen generation. These results will appear in future issues.

4. Conclusions

In this study, chitin–chitinase and collagen–collagenase composites were prepared, and enzyme-based proton production was investigated. It was found that protons can be generated by introducing the enzymes chitinase and collagenase into the substrates chitin

and collagen. The proton concentrations produced by the chitin–chitinase and collagen–collagenase composites were obtained to be $1.68 \times 10^{17} \text{ cm}^{-3}$ and $1.02 \times 10^{17} \text{ cm}^{-3}$, respectively. In addition, the diffusion constants in the chitin and collagen membrane were roughly estimated to be $8.59 \times 10^{-8} \text{ cm}^2/\text{s}$ and $8.69 \times 10^{-8} \text{ cm}^2/\text{s}$, respectively. These results suggest that the composites of hydrolytic enzymes and bio-proton conductors become a new method for achieving proton production. In addition, a biofuel cell was fabricated using chitin–chitinase and collagen–collagenase composites as fuel for the fuel cell, and it was found that protons produced by chitin–chitinase and collagen–collagenase can be used to fuel the fuel cell.

Author Contributions: Conceptualization, H.S., Y.M.; methodology, H.S., Y.M.; formal analysis, H.S., R.Y., Y.M.; investigation, R.Y., H.S., Y.M.; data curation, R.Y., H.S.; writing—original draft preparation, H.S., Y.M.; writing—review and editing, H.S., Y.M.; supervision, H.S., Y.M.; project administration, Y.M.; resources, Y.M. All authors have read and agreed to the published version of the manuscript.

Funding: This research received no external funding.

Conflicts of Interest: The authors declare no conflict of interest.

References

1. Dicks, A.L. Hydrogen generation from natural gas for the fuel cell systems of tomorrow. *J. Power Sources* **1996**, *61*, 113–124. [[CrossRef](#)]
2. Möller, S.; Kaucic, D.; Sattler, C. Hydrogen Production by Solar Reforming of Natural Gas: A Comparison Study of Two Possible Process Configurations. *J. Sol. Energy Eng.* **2006**, *128*, 16–23. [[CrossRef](#)]
3. Lefebvre, C.F.; Abatzoglou, N.; Blanchard, J.; Gitzhofer, F. Steam reforming of liquid hydrocarbons over a nickel–alumina spinel catalyst. *J. Power Sources* **2010**, *195*, 3275–3283. [[CrossRef](#)]
4. Takahashi, Y.; Iwahashi, A.; Matsuo, Y.; Kawakami, H. Solid-State Hydrogen Fuel by PSII–Chitin Composite and Application to Biofuel Cell. *J. Compos. Sci.* **2021**, *5*, 317. [[CrossRef](#)]
5. Hosseini, S.E.; Wahid, M.A. Hydrogen production from renewable and sustainable energy resources: Promising green energy carrier for clean development. *Renew. Sustain. Energ. Rev.* **2016**, *57*, 850–866. [[CrossRef](#)]
6. Andrady, A.L. Microplastics in the marine environment. *Mar. Pollut. Bull.* **2011**, *62*, 1596–1605. [[CrossRef](#)] [[PubMed](#)]
7. Cauwenberghe, L.V.; Janssen, C.R. Microplastics in bivalves cultured for human consumption. *Environ. Pollut.* **2014**, *193*, 65–70. [[CrossRef](#)]
8. Bilo, F.; Pandini, S.; Sartore, L.; Depero, L.E.; Gargiulo, G.; Bonassi, A.; Federici, S.; Bontempi, E. A sustainable bioplastic obtained from rice straw. *J. Clean. Prod.* **2018**, *200*, 357–368. [[CrossRef](#)]
9. Maheswari, N.U.; Ahilandeswari, K. Production of bioplastic using *Spirulina platensis* and comparison with commercial plastic. *Res. Environ. Life Sci.* **2011**, *4*, 133–136.
10. Moorthy, A.G.; Abdul-Latif NI, S.; Ong, M.Y.; Shamsuddin, A.H.; Nomanbhay, S. Enhancement of biodegradability and tensile characteristics of composite plastic film with spirulina algal biomass. *IOP Conf. Ser. Earth Environ. Sci.* **2020**, *476*, 012139. [[CrossRef](#)]
11. Dellago, C.; Naor, M.M.; Hummer, G. Proton transport through water-filled carbon nanotubes. *Phys. Rev. Lett.* **2003**, *90*, 105902. [[CrossRef](#)]
12. Shibata, M.; Enjoji, M.; Sakazume, K.; Ifuku, S. Bio-based epoxy/chitin nanofiber composites cured with amine-type hardeners containing chitosan. *Carbohydr. Polym.* **2016**, *144*, 89–97. [[CrossRef](#)]
13. Matsui, H.; Matsuo, Y. Proton Conduction via Water Bridges Hydrated in the Collagen Film. *J. Funct. Biomater.* **2020**, *11*, 61. [[CrossRef](#)]
14. Matsuo, Y.; Ikeda, H.; Kawabata, T.; Hatori, J.; Oyama, H. Collagen-Based Fuel Cell and Its Proton Transfer. *Mater. Sci. Eng. C* **2017**, *8*, 747–756. [[CrossRef](#)]
15. Kawabata, T.; Matsuo, Y. Chitin Based Fuel Cell and Its Proton Conductivity. *Mater. Sci. Appl.* **2018**, *9*, 779–789. [[CrossRef](#)]
16. Matsuo, Y.; Kumasaka, G.; Saito, K.; Ikehata, S. Fabrication of solid-state fuel cell based on DNA film. *Solid State Commun.* **2005**, *133*, 61–64. [[CrossRef](#)]
17. Furuseki, T.; Matsuo, Y. Fuel Cell Using Squid Axon Electrolyte and Its Proton Conductivity. *J. Funct. Biomater.* **2020**, *11*, 86. [[CrossRef](#)]
18. Zhong, C.; Deng, Y.; Roudsari, A.F.; Kapetanovic, A.; Anantram, M.P.; Rolandi, M. A polysaccharide bioprotonic field-effect transistor. *Nat. Commun.* **2011**, *2*, 476. [[CrossRef](#)] [[PubMed](#)]
19. Park, H.Y.; Dugasani, S.R.; Kang, D.H.; Yoo, G.; Kim, J.; Gnareddy, B.; Jeon, J.; Kim, M.; Song, Y.J.; Lee, S.; et al. M-DNA/Transition Metal Dichalcogenide Hybrid Structurebased Bio-FET sensor with Ultrahigh Sensitivity. *Sci. Rep.* **2016**, *6*, 35733. [[CrossRef](#)]
20. Kirk, O.; Borchert, T.V.; Fuglsang, C.C. Industrial enzyme applications. *Curr. Opin. Biotechnol.* **2002**, *13*, 345–351. [[CrossRef](#)]

21. Galan, C.G.; Murcia, Á.B.; Lafuente, R.F.; Rodrigues, R.C. Potential of Different Enzyme Immobilization Strategies to Improve Enzyme Performance. *Adv. Synth. Catal.* **2011**, *353*, 2885–2904. [[CrossRef](#)]
22. Sathya, T.A.; Khan, M. Diversity of glycosyl hydrolase enzymes from metagenome and their application in food industry. *J. Food Sci.* **2014**, *79*, R2149–R2156. [[CrossRef](#)] [[PubMed](#)]
23. Imig, J.D.; Hammock, B.D. Soluble epoxide hydrolase as a therapeutic target for cardiovascular diseases. *Nat. Rev. Drug Discov.* **2009**, *8*, 794–805. [[CrossRef](#)]
24. Liu, C.; Shi, C.; Zhu, S.; Wei, R.; Yin, C.C. Structural and functional characterization of polyethylene terephthalate hydrolase from *Ideonella sakaiensis*. *Biochem. Biophys. Res. Commun.* **2019**, *508*, 289–294. [[CrossRef](#)]
25. Arakane, Y.; Muthukrishnan, S. Insect chitinase and chitinase-like proteins. *Cell. Mol. Life Sci.* **2010**, *67*, 201–216. [[CrossRef](#)]
26. Perrakis, A.; Tews, I.; Dauter, Z.; Oppenheim, A.B.; Chet, I.; Wilson, K.S.; Constantin, E.V. Crystal structure of a bacterial chitinase at 2.3 Å resolution. *Structure* **1994**, *2*, 1169–1180. [[CrossRef](#)]
27. Fukamizo, T. Chitinolytic enzymes catalysis, substrate binding, and their application. *Curr. Protein Pept. Sci.* **2000**, *1*, 105–124. [[CrossRef](#)]
28. Welgus, H.G.; Jeffrey, J.J.; Eisen, A.Z. The collagen substrate specificity of human skin fibroblast collagenase. *J. Biol. Chem.* **1981**, *256*, 9511–9515. [[CrossRef](#)]
29. Daboor, S.M.; Budge, S.M.; Ghaly, A.E.; Brooks, S.L.; Dave, D. Extraction and Purification of Collagenase Enzymes: A Critical Review. *Am. J. Biochem. Biotechnol.* **2010**, *6*, 239–263. [[CrossRef](#)]
30. De Souza, S.J.; Pereira, H.M.; Jacchieri, S.; Brentani, R.R. Collagen/collagenase interaction: Does the enzyme mimic the conformation of its own substrate? *EASEB J.* **1996**, *10*, 927–930. [[CrossRef](#)]
31. Karthikeyan, C.; Sathishkumar, Y.; Lee, Y.S.; Kim, A.R.; Yoo, D.J.; Kumar, G.G. The Influence of Chitosan Substrate and Its Nanometric Form Toward the Green Power Generation in Sediment Microbial Fuel Cell. *J. Nanosci. Nanotechnol.* **2017**, *17*, 558–563. [[CrossRef](#)]
32. Amine, A.; Mohammadi, H. Amperometry. In *Encyclopedia of Analytical Science*, 2nd ed.; Elsevier: Amsterdam, The Netherlands, 2005; pp. 70–79.
33. Mosharov, E.V.; Sulzer, D. Analysis of exocytotic events recorded by amperometry. *Nat. Methods* **2005**, *2*, 651–658. [[CrossRef](#)]
34. Saveant, J.M.; Vianello, E. Potential-sweep chronoamperometry: Kinetic currents for first-order chemical reaction parallel to electron-transfer process (catalytic currents). *Electrochim. Acta* **1965**, *10*, 905–918. [[CrossRef](#)]
35. Gueshi, T.; Tokuda, K.; Matsuda, H. Voltammetry at partially covered electrodes: Part, I. Chronopotentiometry and chronoamperometry at model electrodes. *J. Electroanal. Chem. Interfacial Electrochem.* **1978**, *89*, 247–260. [[CrossRef](#)]
36. Mostafavi, S.M.; Rouhollahi, A.; Adibi, M.; Pashae, F.; Piryaee, M. Electrochemical Investigation of Thiophene on Glassy Carbon Electrode and Quantitative Determination of it in Simulated Oil Solution by Differential Pulse Voltammetry and Amperometry Techniques. *Asian J. Chem.* **2011**, *23*, 5356–5360.
37. Rong, Z.; Vadgama, P. Bipartite expressions for amperometric currents of recessed, membrane covered planar and hanging mercury drop electrodes. *J. Electroanal. Chem.* **2008**, *614*, 166–170. [[CrossRef](#)]
38. Wang, Y.; Wang, W.; Li, G.; Liu, Q.; Wei, T.; Li, B.; Jiang, C.; Sun, Y. Electrochemical detection of L-cysteine using a glassy carbon electrode modified with a two-dimensional composite prepared from platinum and Fe₃O₄ nanoparticles on reduced graphene oxide. *Mikrochim. Acta* **2016**, *183*, 3221–3228. [[CrossRef](#)]
39. Denuault, G.; Mirkin, M.V.; Bard, A.J. Direct determination of diffusion coefficients by chronoamperometry at microdisk electrodes. *J. Electroanal. Chem. Interfacial Electrochem.* **1991**, *308*, 27–38. [[CrossRef](#)]
40. Hirota, Y.; Tominaga, T.; Kawakita, Y.; Kawabata, T.; Matsuo, Y. Analysis of hydration and dynamics in chitin by neutron inelastic scattering (1). *Nihon Butsuri Gakkai Kouen Gaiyousyu* **2020**, *2*, 75.
41. Shuichi, Y. Diffusion Coefficients as Mass Transfer Properties and Water Ad/Desorption (Drying). *Jpn. J. Food Eng.* **2010**, *11*, 73–85.